AGU PUBLICATIONS

Geophysical Research Letters

RESEARCH LETTER
10.1002/2015GL067619

Key Points:
- Drifter observations and coupled model quantify hurricane impact on surface transport
- Hurricane-induced Stokes drift contributes up to 20% surface current velocity
- Scale-dependent relative diffusivity is estimated to be 6 times larger in hurricanes

Correspondence to:
S. S. Chen,
schen@rsmas.miami.edu

Citation:
Curcic, M., S. S. Chen, and T. M. Özgökmen (2016), Hurricane-induced ocean waves and stokes drift and their impacts on surface transport and dispersion in the Gulf of Mexico, *Geophys. Res. Lett.*, *43*, doi:10.1002/2015GL067619.

Received 30 DEC 2015
Accepted 4 FEB 2016
Accepted article online 9 FEB 2016

Hurricane-induced ocean waves and stokes drift and their impacts on surface transport and dispersion in the Gulf of Mexico

Milan Curcic[1], Shuyi S. Chen[1], and Tamay M. Özgökmen[1]

[1]Rosenstiel School of Marine and Atmospheric Sciences, University of Miami, Coral Gables, Florida, USA

Abstract Hurricane Isaac induced large surface waves and a significant change in upper ocean circulation in the Gulf of Mexico before making landfall at the Louisiana coast on 29 August 2012. Isaac was observed by 194 surface drifters during the Grand Lagrangian Deployment (GLAD). A coupled atmosphere-wave-ocean model was used to forecast hurricane impacts during GLAD. The coupled model and drifter observations provide an unprecedented opportunity to study the impacts of hurricane-induced Stokes drift on ocean surface currents. The Stokes drift induced a cyclonic (anticyclonic) rotational flow on the left (right) side of the hurricane and accounted for up to 20% of the average Lagrangian velocity. In a significant deviation from drifter measurements prior to Isaac, the scale-dependent relative diffusivity is estimated to be 6 times larger during the hurricane, which represents a deviation from Okubo's (1971) canonical results for lateral dispersion in nonhurricane conditions at the ocean surface.

1. Introduction

Hurricanes produce extremely high winds and waves, which have a significant impact on the upper ocean circulation and water mass transport. It is important to develop a better understanding and prediction of hurricane impacts in events such as the Deepwater Horizon oil spill in the Gulf of Mexico in 2010 [*Crone and Tolstoy*, 2010]. Ocean surface waves induce a mass transport in the direction of their propagation [*Longuet-Higgins*, 1953]. It is commonly referred to as Stokes drift, named after *Stokes* [1847], which can be computed from the wave energy spectrum. *Kenyon* [1969] estimated the magnitude of the Stokes drift based on wind speed in a simple steady state case that had no verification from the observations. Others used parameterized equilibrium spectra and integrated quantities such as significant wave height and mean period [*Webb and Fox-Kemper*, 2011], which may significantly overestimate the Stokes drift without the consideration of directional and frequency spreading of the spectrum [*Webb and Fox-Kemper*, 2015]. *Röhrs et al.* [2012] found the impacts of Stokes drift to be of the same order of magnitude as Eulerian currents based on observations on the continental shelf waters of Norway. Recent studies showed the importance of Stokes drift in local upper ocean circulation in hurricane conditions [*Sullivan et al.*, 2012; *Rabe et al.*, 2015]. However, the effects of the Stokes drift on storm-scale horizontal surface current in hurricanes have not been studied by in situ observations and coupled modeling.

Although direct measurements of Stokes drift are difficult to obtain from the surface waves in the field, especially in high wind conditions such as in hurricanes and winter storms, *D'Asaro* [2015] had some success deriving it using subsurface floats. Surface wave effects are not included in existing operational ocean circulation models [e.g., *Chassignet et al.*, 2009]. Recent advancement in high-resolution, fully coupled atmosphere-wave-ocean modeling made it possible to study the hurricane-induced surface waves and Stokes drift. *Chen and Curcic* [2016] showed that the coupled model predictions of ocean surface waves in Hurricane Ike (2008) and Superstorm Sandy (2012) were verified very well against both in situ observations from the National Data Buoy Center buoys and the satellite observations. The coupled modeling studies by *Chen et al.* [2013] and *Chen and Curcic* [2016] have shown that hurricane-induced surface waves are highly complex and asymmetric in terms of wave heights and propagation directions around a moving storm. However, direct measurements of the surface currents are needed to examine the impacts of the waves and the Stokes drift on the ocean surface mass transport.

In response to the recent oil spill events, the Grand Lagrangian Deployment (GLAD) field campaign was carried out in the Gulf of Mexico in July–August of 2012, during which nearly 300 surface drifters were deployed to capture the surface transport and dispersion dynamics in both submesoscale and mesoscale ocean circulation regimes [*Poje et al.*, 2014; *Olascoaga et al.*, 2013]. One of the objectives of GLAD was to observe upper

ocean circulation under various weather conditions, including hurricanes. Hurricane Isaac developed over the Western Atlantic-Caribbean regions and propagated through the Gulf of Mexico before it made landfall near the Louisiana coast on 29 August 2012. One hundred ninety-four of the GLAD drifters were subjected to strong wind and wave forcing induced by Isaac and provided an unprecedented near-surface Lagrangian velocity with high spatial and temporal resolution under the hurricane conditions. During GLAD, the coupled atmosphere-wave-ocean model, as described in *Chen and Curcic* [2016], was used for forecasting the atmospheric and ocean conditions in support of the field program. It provided high-resolution forecast fields of wind, waves, and ocean currents in Hurricane Isaac.

One of the primary outcomes of the GLAD program was that during the period before Hurricane Isaac, two-point dispersion statistics in the upper ocean were found to be local, driven predominantly by the energetic submesoscale fluctuations [*Poje et al*., 2014]. In particular, the scale-dependent relative diffusivity K_{eff} to describe lateral material spreading, was shown to scale as $K_{\text{eff}} \sim L^{4/3}$, as predicted in the seminal work by *Richardson* [1926], as well as in accordance with canonical observations taken in various lakes and oceans [*Okubo*, 1971]. The Richardson's four-thirds law is fundamentally consistent with the turbulence theory by *Kolmogorov* [1941], which has a rather striking generality applicable from 3-D small-scale turbulence to tens of kilometers in the ocean. A question remains whether this scaling is valid in the ocean under all weather conditions.

This study addresses two hypotheses: First, we suspect that the hurricane-induced Stokes drift will have a large impact on the near-surface ocean currents. Second, we presume that the generality of *Richardson* [1926] and *Okubo* [1971] results will be challenged under hurricane conditions. We present the analysis to explore these hypotheses, using the unique GLAD drifter data and the coupled model. Sections 2 and 3 provide descriptions of the GLAD drifter measurements and the coupled model, respectively. The analysis of the Stokes drift and its impacts on the surface mass transport in Hurricane Isaac (2012) are presented in section 4. Section 5 discusses the implication of the Stokes drift on water mass displacement and dispersion. Finally, conclusions are given in section 6.

2. GLAD Drifter Measurements

The GLAD drifters have a similar design as those used in the Coastal Ocean Dynamics Experiment [*Davis*, 1985] with a drogue at 1 m depth. The positions were recorded using the Global Positioning System at 5 min intervals with an accuracy of about 5 m. *Coelho et al*. [2015] processed the raw position data to obtain quality-controlled estimates of Lagrangian velocity $\mathbf{u}_L$ at 15 min intervals. This velocity consists of contributions from Eulerian velocity $\mathbf{u}_E$ and Stokes drift $\mathbf{u}_{\text{St}}$, such that $\mathbf{u}_L = \mathbf{u}_E + \mathbf{u}_{\text{St}}$ [*Craik*, 1982; *McWilliams et al*., 2004]. $\mathbf{u}_E$ is the mean current that represents barotropic and baroclinic ocean circulation on time scales considerably longer than the surface gravity wave period. $\mathbf{u}_{\text{St}}$ is a residual drift that arises due to material orbits not being closed under a wavy water surface [*Phillips*, 1977], which is implicitly measured by the drifters. However, it is difficult to decompose $\mathbf{u}_E$ and $\mathbf{u}_{\text{St}}$ from the drifter measurement alone without direct observation of the surface waves. We assume that direct wind forcing on the drifter is negligible relative to the wind forcing on the water surrounding the drogue. The GLAD data used in this study are available publically [*Özgökmen*, 2013].

3. Coupled Atmosphere-Wave-Ocean Model

The coupled atmosphere-wave-ocean model used in this study is the Unified Wave INterface-Coupled Model (UWIN-CM) [*Chen et al*., 2013; *Chen and Curcic*, 2016]. The components of UWIN-CM are the Weather Research and Forecasting (WRF) [*Skamarock et al*., 2008] model for the atmosphere, University of Miami Wave Model (UMWM) [*Donelan et al*., 2012] for the ocean surface waves, and HYbrid Coordinate Ocean Model (HYCOM) [*Wallcraft et al*., 2009] for the ocean circulation. The WRF model is configured with nested grids of 12, 4, and 1.3 km horizontal grid spacing, respectively, and 36 vertical levels. The outermost WRF model domain is from 55.0–103.0 W in longitude to 7.0–45.0 N in latitude. The two inner nested grids are storm following. Both UMWM and HYCOM domains cover the same region as the WRF outermost domain but with a 4 km and 0.04 horizontal grid spacing, respectively. HYCOM has 32 vertical levels with the top three layers centered at 1.5, 4.8, and 8.6 m depth. We use the nonlocal K profile vertical mixing scheme [*Large et al*., 1994] in HYCOM. UMWM resolves wave frequencies from 0.0313 to 2 Hz with 36 directional bins, which allows for a broad range of wave states in hurricane conditions.

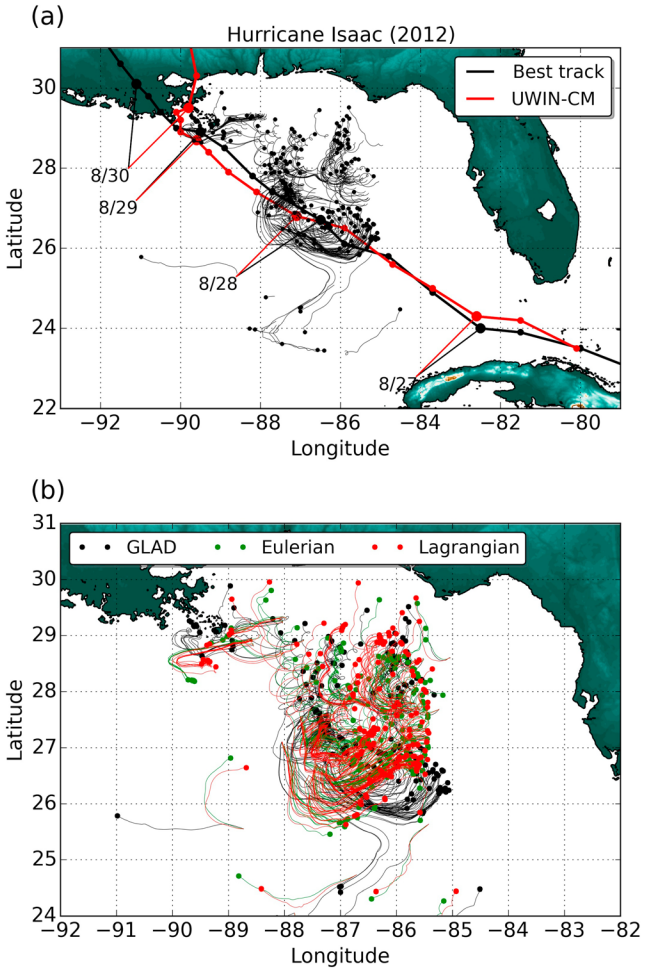

Figure 1. (a) The NHC best track (thick black line) and UWIN-CM forecast track (red line) of Hurricane Isaac from 1200 UTC 26 August to 0000 UTC 31 August. GLAD drifter trajectories (thin black lines) during the same time period of the Hurricane Isaac passage with the end positions marked by black dots. (b) GLAD drifters (black) and UWIN-CM trajectories computed using Eulerian (green) and Lagrangian (red) velocities started at the same initial positions as the GLAD drifters.

The wind-wave-current coupling concept used in UWIN was described in *Chen et al.* [2013]. However, the component models in UWIN-CM are different, which were described in *Chen and Curcic* [2016]. Another advancement of UWIN-CM is the explicit momentum coupling through waves. Instead of using wind stress, the wave dissipation computed from UMWM is used to compute current stress. Although the surface current is used as input for the wave model, the wave drift is not explicitly coupled with the current field. The HYCOM surface current is used to compute the Eulerian velocity $\mathbf{u}_E$. The Stokes drift velocity $\mathbf{u}_{St}$ is computed from the UMWM by integrating the third moment of the wave variance spectrum over the explicitly resolved frequency range (0.0313–2 Hz). We then use these modeled velocity fields to compute the particle trajectory in time from UWIN-CM output to compare with the GLAD drifter Lagrangian velocity measurements. While the Eulerian velocity may be modulated by Coriolis-Stokes [*Polton et al.*, 2005] and vortex forces [*Craik and Leibovich*, 1976], these processes are not represented in the model. Here we focus solely on the advection by the Stokes drift.

The initial and lateral boundary conditions for the atmosphere and ocean components of UWIN-CM were provided by the National Center for Environmental Prediction Global Forecasting System 6-hourly forecast fields (0.25 grid spacing) and the global HYCOM daily forecast fields (0.08 grid spacing), respectively. The UWIN-CM 5 day forecast of Hurricane Isaac was initialized at 1200 UTC on 26 August 2012.

4. Stokes Drift and Ocean Transport in Hurricane Isaac

Hurricane Isaac entered the Gulf of Mexico as a tropical storm on at 0000 UTC in 27 August and intensified to a Category 1 hurricane at 1800 UTC in 28 August, reaching a peak wind speed at 70 kts before making landfall at 0800 UTC in 29 August [*Berg*, 2013]. The UWIN-CM forecast of Hurricane Isaac track is similar to the National Hurricane Center (NHC) best track over the Gulf (Figure 1a). Isaac propagated through the area populated by GLAD drifters in August 28. Most drifters on the left side of the storm were first pushed toward southeast and then toward northeast across the storm track. The drifters on the right side exhibited predominantly anticyclonic trajectories with strong inertial oscillations in the Isaac's wake.

We construct two synthetic drifter data sets from UWIN-CM by sampling the same initial locations as the GLAD drifters; one using the Eulerian velocity field $\mathbf{u}_E$, and another using the Lagrangian velocity field $\mathbf{u}_L = \mathbf{u}_E + \mathbf{u}_{St}$. In deep water, the Stokes drift decays exponentially with depth and is computed as: $\mathbf{u}_{st} = 2 \iint \omega \mathbf{k} e^{2kz} F \, dk \, d\theta$, where ω is the radian frequency of the surface waves; $\mathbf{k}$ is the directional

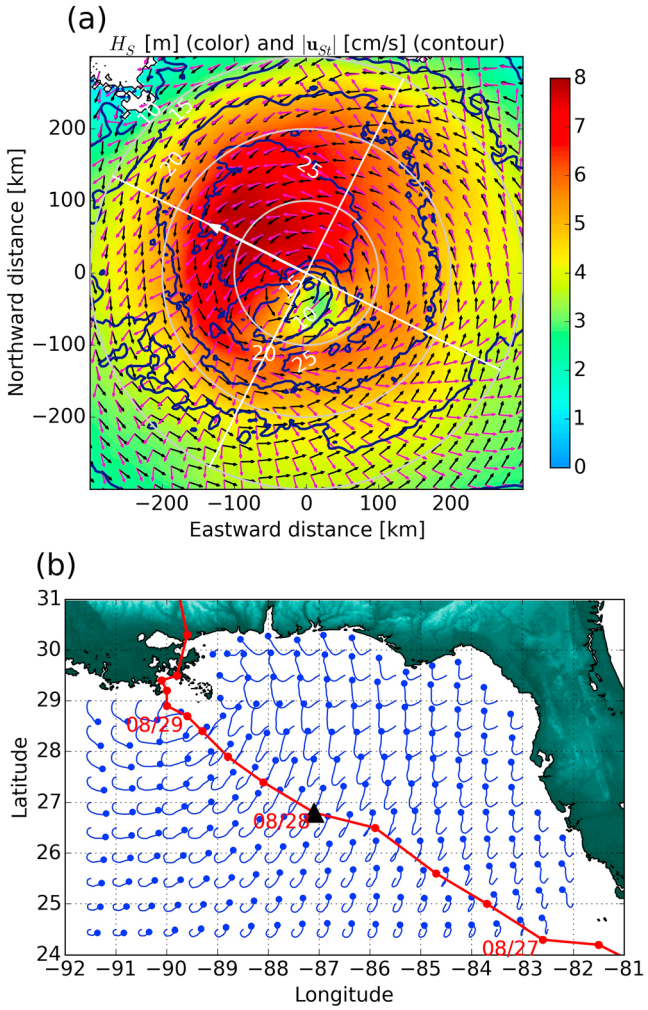

Figure 2. (a) Significant wave height (color shading) and surface Stokes drift (contour) in Hurricane Isaac at 0000 UTC on 28 August 2012. Black and magenta vectors indicate wind and dominant wave directions, respectively. The white arrow indicates the direction of storm motion, while the gray circles mark the distance from the storm center at 100, 200, and 300 km. (b) UWIN-CM particle trajectories advected by the Stokes drift, starting at 1200 UTC in 26 August. The dots mark the end positions at 0000 UTC in 31 August. The red line is the model track of Hurricane Isaac. The black triangle indicates the storm center shown in Figure 2a.

wavenumber; θ is the wave direction; z is the displacement from the surface; and F is the wave spectrum. $\mathbf{u}_E$ is computed as the velocity of the first HYCOM layer of 3 m depth. $\mathbf{u}_{St}$ is vertically averaged over the upper 1 m, mimicking the depth of the GLAD drifter drogues. The release time for the synthetic drifters is when direct forcing by Hurricane Isaac began at 0000 UTC in 27 August (Figure 1b).

To examine the storm-induced Stokes drift and its impact on the water mass transport, we compute the $\mathbf{u}_{St}$-induced trajectories from UWIN-CM from prior- to post-storm conditions from 1200 UTC 26 August to 0000 UTC 31 August (Figure 2). At 0000 UTC in 28 August, the waves are highest in the front-right quadrant of the storm due to resonance with storm motion, with the significant wave height exceeding 8 m (Figure 2a). The dominant wave direction is almost parallel with the wind on the right side of the storm and is oriented outward on the left side. The Stokes drift is largest in the front-right quadrant where the waves are highest, exceeding 0.25 m s^{-1}. The Stokes drift trajectories show a clear asymmetry with respect to the storm track: cyclonic (anticyclonic) on the left (right) side of the storm (Figure 2b). These trajectories reflect the characteristics of the surface waves forced by cyclonic winds in the hurricane. As the storm approaches, the water surface is displaced to the left in front of the storm; during the storm passage over the area, it is displaced backward on the left side and forward on the right side; finally, in the rear of the storm, it is displaced

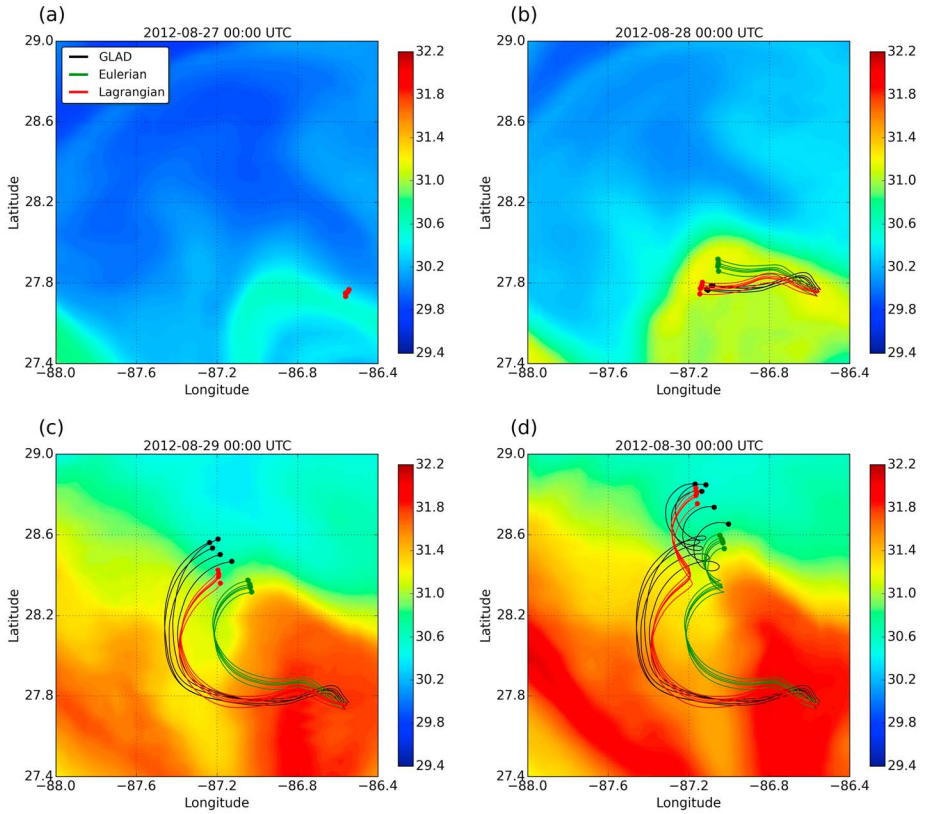

Figure 3. (a–d) Trajectories of a five member cluster located in a strongly forced region on the right side of Hurricane Isaac track from 0000 UTC 27 to 30 August 2012. GLAD drifter (black) and UWIN-CM trajectories computed using the Eulerian (green) and Lagrangian (red) velocities started at the same initial positions as the GLAD drifters. The dots mark drifter locations valid on the time indicated on top of each panel. The color background shows surface seawater density ($\times 1000\,\mathrm{kg\,m^{-3}}$) from the coupled model.

across the track toward the right. The distance that the particles traveled during the 4.5 day period of Isaac ranges from 35 to 109 km, with an average value of 70 km and a standard deviation of 16 km. The average Stokes velocity during Isaac's passage ranged from 0.09 to $0.28\,\mathrm{m\,s^{-1}}$, with an average value of $0.18\,\mathrm{m\,s^{-1}}$ and a standard deviation of $0.04\,\mathrm{m\,s^{-1}}$.

The impact of the Stokes drift on the ocean surface circulation is well illustrated by the difference between the trajectories computed using the Eulerian and Lagrangian velocities using a group of five model-simulated drifters from the same initial positions as the GLAD drifters located on the right side of the storm track of Hurricane Isaac, where the storm-induced inertial current is strong (Figure 3). Average distances traveled by the five drifter groups were 229 km for the GLAD drifters, 196 km for the model-simulated Lagrangian, and 153 km for Eulerian currents.

The net effect of the Stokes drift on the basin-scale near-surface current is summarized by averaging the Lagrangian, Eulerian, and Stokes drift velocities of all GLAD drifters and UWIN-CM-simulated fields sampled along the drifter trajectories (Figure 4), which can be expressed as $<|\mathbf{u}_L|>$, $<|\mathbf{u}_E|>$, and $<|\mathbf{u}_{St}|>$, respectively. The observed mean Lagrangian current $<|\mathbf{u}_L|>$ averaged over all the GLAD drifters in the Gulf (Figure 1a) increased from about $0.4\,\mathrm{m\,s^{-1}}$ prior to the passage of Hurricane Isaac at 1200 UTC 26 August to more than $1.0\,\mathrm{m\,s^{-1}}$ when the center of Isaac was over the drifter array in 28 August (Figure 4a). The model-simulated mean Eulerian current $<|\mathbf{u}_E|>$ computed from HYCOM varied from 0.3 to $0.8\,\mathrm{m\,s^{-1}}$ during Isaac, which is ~20% less than the surface current observed by the GLAD drifters. The mean Stokes drift velocity $<|\mathbf{u}_{St}|>$ computed from the UMWM exceeds $0.2\,\mathrm{m\,s^{-1}}$ at the time of the strongest wind forcing. The highest Stokes drift magnitude sampled at GLAD locations was $0.44\,\mathrm{m\,s^{-1}}$ (Figure 4a). The UWIN-CM simulated $<|\mathbf{u}_L|>$, which is the sum of the vectors of Eulerian and Stokes current, is in a much better agreement with that observed from

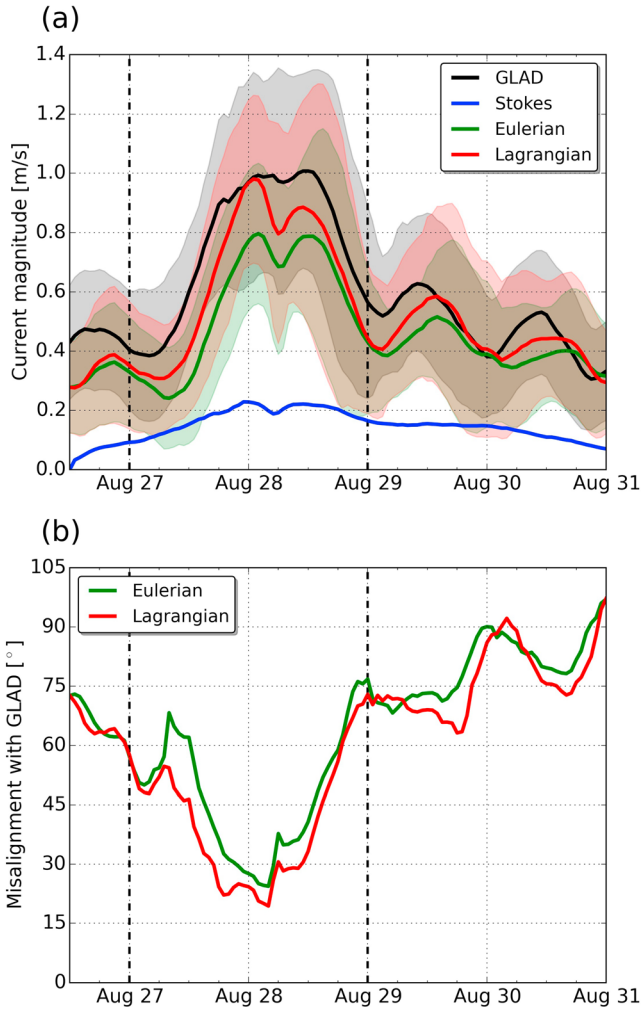

Figure 4. (a) The upper 1 m velocity magnitude averaged over the entire GLAD data set. The shading indicates the width of 2 standard deviations. The Stokes (blue), Eulerian (green), and Lagrangian (red) components are obtained by sampling the model fields at the positions of each GLAD drifter. (b) Average misalignment angle between modeled and GLAD velocities, in case of Eulerian (green) and Lagrangian (red) velocity. Dashed lines mark the times when Hurricane Isaac approached the drifters and when it made landfall.

GLAD drifters than $<|\mathbf{u}_E|>$. The local $<|\mathbf{u}_L|>$ minimum at 0600 UTC in 28 August is associated with the passage of the eye of Hurricane Isaac, where the wind, waves, and Eulerian current are considerably lower relative to the surrounding eyewall region. The slight decrease in $<|\mathbf{u}_{St}|>$ in the eye suggests that $<|\mathbf{u}_{St}|>$ is dominated by swell rather than wind waves. This minimum is more pronounced in the model than in GLAD data, indicating that either the size of the eye may be larger in the model or it was not fully resolved by the limited number of drifters in the inner core region of the storm. The standard deviation of the simulated Lagrangian current (0.28 m s^{-1} at peak) is increased compared to the Eulerian current (0.23 m s^{-1} at peak) but underestimated compared to GLAD (0.35 m s^{-1} at peak). As soon as Isaac passed the drifter array at 0000 UTC in 29 August, inertial oscillations started dominating the circulation, as is evident from both observed and modeled $<|\mathbf{u}_L|>$. The magnitude of the inertial currents was enhanced by the Stokes drift from 29 to 30 August, which matches the GLAD observation better than the model-simulated Eulerian current (Figure 4a). The average misalignment between the model simulated and observed velocities was less than 90° during most of the period and was smallest at the peak of the hurricane wind forcing (Figure 4b). The Stokes drift $<|\mathbf{u}_{St}|>$ contributed approximately 20% of the total Lagrangian velocity on average. Overall, including the Stokes drift in the model improves the estimate of magnitude, direction, and variability of near-surface currents during Hurricane Isaac.

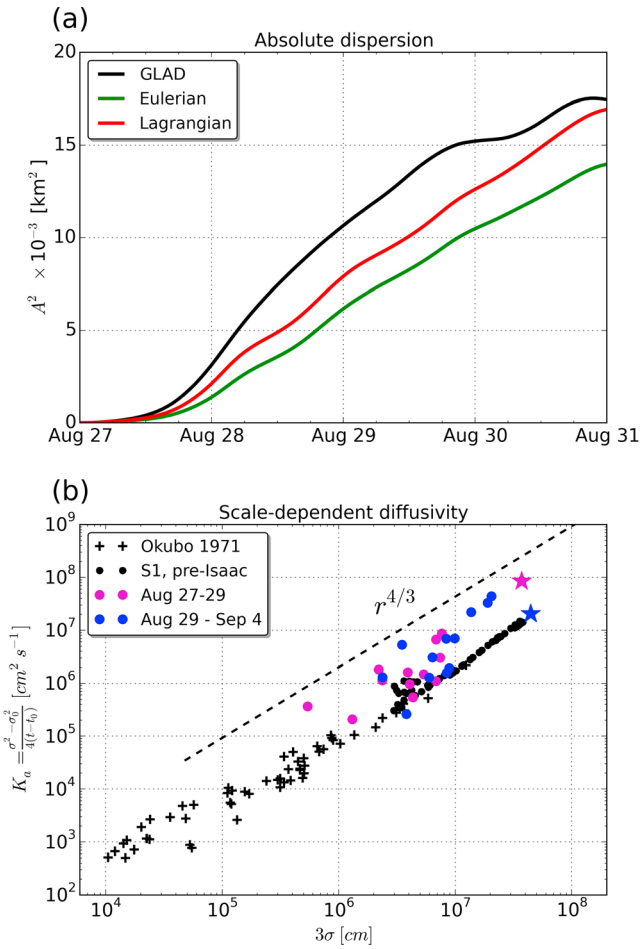

Figure 5. (a) Absolute dispersion A^2 computed from GLAD (black) and modeled Eulerian (green) and Lagrangian (red) velocity fields. (b) Relative diffusivity as function of separation scale, based on ellipse fitting to groups of GLAD drifters during Hurricane Isaac forcing from 27 to 29 August (magenta dots), and after Hurricane Isaac from 29 August to 4 September (blue dots). The stars are diffusivities computed using the entire GLAD drifter set. Black dots are prestorm diffusivities obtained from the S1 deployment in GLAD and extended from the data shown in *Poje et al*. [2014]. Black pluses are the results of *Okubo* [1971]. The dashed line indicates *Richardson*'s [1926] 4/3 power law. Separation scale ranges from 5 to 373 km.

5. Horizontal Dispersion

Intrinsic to the transport problem are the absolute displacement (translation) of particles from their location of origin and the spreading (separation) of particles relative to each other. The former may be quantified by the absolute dispersion $A^2(t) = <(\mathbf{x}(t) - \mathbf{x}(0))^2>$ [*Taylor*, 1921], while the latter is commonly quantified by relative dispersion $D^2(t) = <(\mathbf{x}_m(t) - \mathbf{x}_n(t))^2>$, for all particle pairs m, n such that $m \neq n$ [e.g., *Batchelor*, 1952]. A^2 is often not considered in calm winds when only the particle separation times at different spatial scales are of interest [*Poje et al*., 2014]. However, in strong wind forcing such as hurricanes, absolute displacement may be the dominant mode of transport. During Hurricane Isaac, GLAD drifters experience strong increase in A^2 (Figure 5a), being displaced from their initial locations by over 130 km on average. The absolute dispersion coefficient, defined as $1/2\ dA^2/dt$ [e.g., *Haza et al*., 2012], peaks at the time of strongest wind in early morning of August 28 and equals $0.56 \times 10^5\ m^2\ s^{-1}$ in case of GLAD, $0.43 \times 10^5\ m^2\ s^{-1}$ in case of simulated Lagrangian current trajectories, and $0.30 \times 10^5\ m^2\ s^{-1}$ in case of simulated Eulerian current trajectories (not shown).

Following *Okubo* [1971], who compiled a large number of dye release experiments, we compute the scale-dependent relative diffusivity by fitting ellipses to the surface area covered by the drifters, $\sigma^2 = 2\sigma_a\sigma_b$, where σ_a and σ_b are the major and minor semiaxes of the ellipse, respectively. The length scale representative of the drifter cloud is $L = 3\sigma$, and the diffusivity is $K_{eff} = ¼\ (\sigma^2(t) - \sigma^2(t_0))/(t - t_0)$ [*Peeters and Hofmann*, 2015]. The positions of GLAD drifters at the time of Isaac passage allow us to estimate diffusivity from nearly submesoscales

(~5 km) to the hurricane vortex scale (>350 km). K_{eff} measured by GLAD drifters during the 2 days of Isaac's direct forcing (27–29 August) is increased by a factor of 6 relative to those before Isaac (Figure 5b), in comparison to the results reported in *Poje et al*. [2014]. While direct hurricane forcing disperses material mainly on the hurricane scale, smaller scales become significantly more dispersive after the passage of the storm. The post-Isaac diffusivity at the largest scale (blue star), which corresponds to the whole GLAD set, is in line with the canonical results of *Okubo* [1971] and pre-Isaac estimates of *Poje et al*. [2014].

To further investigate the physical processes governing the spread of the particles during and after the hurricane passage, we found that density fronts form in hurricane-induced cold wake (Figure 3). The mixed layer eddies (MLEs) play an important role in restratification through adjustment process as described by *Fox-Kemper et al*. [2008], which are ageostrophic, baroclinic, and exclusively submesoscale from O(100 m) to O (10 km). MLEs were found to dominate the adjustment over other restratification mechanisms in idealized submesoscale-resolving simulations by *Haney et al*. [2012], when the cold wake is deep and narrow. In Isaac, the most strongly forced drifters were found on the right side of the storm in the region of the density fronts associated with the storm-induced cold wake (Figure 3). While the absolute displacement can be well reproduced in the coupled model if the Stokes drift is included, the relative spreading of the group was underpredicted on and after August 29 (Figures 3c and 3d). This is expected given the relatively coarse horizontal resolution in HYCOM, which cannot resolve the submesoscale dynamics. Local surface density increase is associated with strong mixing and upwelling in Isaac's wake (approximately −2 C surface temperature anomaly), leading to the formation of a strong horizontal density front. During the restratification process, the GLAD drifters were subjected to vigorous submesoscale dispersion, as shown in Figure 5b.

6. Conclusions

The in situ observations by the GLAD drifters and the high-resolution coupled model UWIN-CM provided a rare opportunity to study the Stokes drift associated with the ocean surface waves and its impacts on the near-surface water mass transport under hurricane conditions over the Gulf of Mexico. The Stokes drift contributed significantly to surface transport during Hurricane Isaac. The spatial structure of the Stokes drift is closely related to the structure of surface winds and direction of the storm motion, mainly enhancing shoreward and cross-track surface transport on the right side of the storm. The resulting wave-induced trajectories are cyclonic on the left side of the storm track and anticyclonic on the right side. During the strong wind forcing in Isaac, the Stokes drift contributes to about 20% of the Lagrangian flow magnitude on average, and changes its orientation by up to 20°. The Eulerian current from the ocean circulation models like HYCOM underestimates the near-surface water mass transport in strong wind conditions as confirmed by the GLAD drifter measurements. Consistent with the hypotheses posed in this study, our results suggest that the Stokes drift should be included in the model prediction of the upper ocean transport in the event of an oil spill or other pollutant, especially in high-wind conditions such as hurricanes or winter storms. The results also provide rare evidence of significant deviations from Richardson's 4/3 law and *Okubo*'s [1971] canonical results for lateral dispersion at the ocean surface under a hurricane. Interestingly, the posthurricane period is characterized by the enhanced relative diffusivity across a broadband of length scales, which is likely due to strong submesoscale adjustment during the upper ocean restratification in the wake of the storm.

Acknowledgments
We thank Andrew C. Poje for providing analysis code to reproduce his results. Comments and suggestions from two anonymous reviewers have helped improve the manuscript. This research was made possible in part by a grant from BP/The Gulf of Mexico Research Initiative and in part by a research grant by the Office of Naval Research under the National Oceanography Partnership Program (N0001401010162).

References

Batchelor, G. K. (1952), Diffusion in a field of homogeneous turbulence, II: The relative motion of particles, *Proc. Cambridge Philos. Soc.*, *48*, 345–362.
Berg, R. (2013), Tropical Cyclone Report Hurricane Isaac (AL092012), NHC. [Available at http://www.nhc.noaa.gov/data/tcr/AL092012_Isaac.pdf.]
Chassignet, E. P., et al. (2009), U.S. GODAE: Global ocean prediction with the HYbrid Coordinate Ocean Model (HYCOM), *Oceanography*, *22*, 64–75.
Chen, S. S., and M. Curcic (2016), Ocean surface waves in Hurricane Ike (2008) and Superstorm Sandy (2012): Coupled modeling and observations, *Ocean Model.*, doi:10.1016/j.ocemod.2015.08.005, in press.
Chen, S. S., W. Zhao, M. A. Donelan, and H. L. Tolman (2013), Directional wind-wave coupling in fully coupled atmosphere-wave-ocean models: Results from CBLAST-Hurricane, *J. Atmos. Sci.*, *70*, 3198–3215.
Coelho, E. F., et al. (2015), Ocean currents estimation using a multi-model ensemble Kalman filter during the Grand Lagrangian Deployment, *Ocean Model.*, *87*, 86–106.
Craik, A. D. D. (1982), The drift velocity of water waves, *J. Fluid Mech.*, *116*, 187–205.
Craik, A. D. D., and S. Leibovich (1976), A rational model for Langmuir circulations, *J. Fluid Mech.*, *73*(03), 401–426.
Crone, T. J., and M. Tolstoy (2010), Magnitude of the 2010 Gulf of Mexico oil leak, *Science*, *330*(6004), 634.
D'Asaro, E. A. (2015), Surface wave measurements from subsurface floats, *J. Atmos. Oceanic Technol.*, *32*, 816–827.

Davis, R. (1985), Drifter observations of coastal surface currents during CODE: The method and descriptive view, *J. Geophys. Res.*, *90*, 4741–4755, doi:10.1029/JC090iC03p04741.
Donelan, M. A., M. Curcic, S. S. Chen, and A. K. Magnusson (2012), Modeling waves and wind stress, *J. Geophys. Res.*, *117*, C00J23, doi:10.1029/2011JC007787.
Fox-Kemper, B., R. Ferrari, and R. Hallberg (2008), Parameterization of mixed layer eddies. Part I: Theory and diagnosis, *J. Phys. Oceanogr.*, *38*, 1145–1165.
Haney, S., S. Bachman, B. Cooper, S. Kupper, K. McCaffrey, L. V. Roekel, S. Stevenson, B. Fox-Kemper, and R. Ferrari (2012), Hurricane wake restratification rates of one-, two- and three-dimensional processes, *J. Mar. Res.*, *70*, 824–850.
Haza, A. C., T. M. Özgökmen, A. Griffa, Z. D. Garraffo, and L. Piterbarg (2012), Parameterization of particle transport at submesoscales in the Gulf Stream region using Lagrangian subgridscale models, *Ocean Model.*, *42*, 31–49.
Kenyon, K. E. (1969), Stokes drift for random gravity waves, *J. Geophys. Res.*, *74*, 6991–6994, doi:10.1029/JC074i028p06991.
Kolmogorov, A. (1941), Dissipation of energy in locally isotropic turbulence, *Proc. Math. Phys. Sci.*, *434*(1890), 15–17.
Large, W. G., J. C. McWilliams, and S. C. Doney (1994), Oceanic vertical mixing: A review and a model with a nonlocal boundary layer parameterization, *Rev. Geophys.*, *32*, 363–403, doi:10.1029/94RG01872.
Longuet-Higgins, M. S. (1953), Mass transport in water waves, *Philos. Trans. R. Soc. London*, *245*, 535–581.
McWilliams, J. C., J. M. Restrepo, and E. M. Lane (2004), An asymptotic theory for the interaction of waves and currents in coastal waters, *J. Fluid Mech.*, *511*, 135–178.
Okubo, A. (1971), Oceanic diffusion diagrams, *Deep-Sea Res.*, *18*, 789–802.
Olascoaga, M. J., et al. (2013), Drifter motion in the Gulf of Mexico constrained by altimentric Lagrangian coherent structures, *Geophys. Res. Lett.*, *40*, 6171–6175, doi:10.1002/2013GL058624.
Özgökmen, T. M. (2013), CARTHE: GLAD experiment CODE-style drifter trajectories (low-pass filtered, 15 minute interval records), northern Gulf of Mexico near DeSoto Canyon, July–October 2012. Distributed by: Gulf of Mexico Research Initiative Information and Data Cooperative (GRIIDC), Harte Research Institute, Texas A&M University-Corpus Christi. doi:10.7266/N7VD6WC8. [Available at https://data.gulfresearchinitiative.org/data/R1.x134.073:0004/.]
Peeters, F., and H. Hofmann (2015), Length-scale dependence of horizontal dispersion in the surface water of lakes, *Limnol. Oceanogr.*, doi:10.1002/lno.10141.
Phillips, O. M. (1977), *Dynamics of the Upper Ocean*, Cambridge Univ. Press, Cambridge, U. K.
Poje, A. C., et al. (2014), Submesoscale dispersion in the vicinity of the Deepwater Horizon spill, *Proc. Natl. Acad. Sci. U.S.A.*, *111*(12), 12,693–12,698.
Polton, J. A., D. M. Lewis, and S. E. Belcher (2005), The role of wave-induced Coriolis-Stokes forcing on the wind-driven mixed layer, *J. Phys. Oceanogr.*, *35*(4), 444–457.
Rabe, T. J., T. Kukulka, I. Ginis, T. Hara, B. G. Reichl, E. A. D'Asaro, R. R. Harcourt, and P. P. Sullivan (2015), Langmuir turbulence under hurricane gustav (2008), *J. Phys. Oceanog.*, *45*(3), 657–677.
Richardson, L. F. (1926), Atmospheric diffusion shown on a distance-neighbour graph, *Proc. R. Soc. London Ser. A*, *110*, 709–737.
Röhrs, J., K. H. Christensen, L. R. Hole, G. Broström, M. Drivdal, and S. Sundby (2012), Observation-based evaluation of surface wave effects on currents and trajectory forecasts, *Ocean Dyn.*, *62*, 1512–1533.
Skamarock, W. C., J. B. Klemp, J. Dudhia, D. Gill, D. Barker, M. Duda, X.-Y. Huang, W. Wang, and J. G. Powers (2008), A description of the Advanced Research WRF Version 3, *Tech. Rep.*, NCAR Technical Note NCAR/TN-475 + STR.
Stokes, G. G. (1847), On the theory of oscillatory waves, *Trans. Cambrige Philos. Soc.*, *8*, 441.
Sullivan, P. P., L. Romero, J. C. McWilliams, and W. K. Melville (2012), Transient evolution of langmuir turbulence in ocean boundary layers driven by hurricane winds and waves, *J. Phys. Oceanog.*, *42*(11), 1959–1980.
Taylor, G. I. (1921), Diffusion by continuous movements, *Proc. Lond. Math. Soc.*, *20*, 196–212.
Wallcraft, A. J., E. J. Metzger, and S. N. Carroll (2009), Software design description for the HYbrid Coordinate Ocean Model (HYCOM) version 2.2, *Tech. Rep.*, NRL/MR/732009-9166.
Webb, A., and B. Fox-Kemper (2011), Wave spectral moments and Stokes drift estimation, *Ocean Model.*, *40*, 273–288.
Webb, A., and B. Fox-Kemper (2015), Impacts of wave spreading and multidirectional waves on estimating Stokes drift, *Ocean Model.*, *96*, 49–64.